8TH INTERNATIONAL SYMPOSIUM ON PARTICLE IMAGE VELOCIMETRY - PIV09
Melbourne, Victoria, Australia, August 25-28, 2009

In-vivo Synchrotron PIV for the measurement of airway motion

A.Fouras[1;2], S. Dubsky[1;2], J. Nguyen[1;2], K. Hourigan[1;2], M.J. Kitchen[3], B.J.Allison[4], M.J.Wallace[4], M.L.Siew[4], K.K.W. Siu[3;5], R.A. Lewis[5], K. Uesugi[6], N. Yagi[6], S.B. Hooper[4]

[1]Division of Biological Engineering, Monash University, VIC 3800, AUSTRALIA

fouras@eng.monash.edu

[2]Fluids Laboratory for Aeronautical and Industrial Research (FLAIR), Department of Mechanical and Aerospace Engineering, Monash University, VIC 3800, AUSTRALIA

[3]School of Physics, Monash University, VIC 3800, AUSTRALIA

[4]Department of Physiology, Monash University, VIC 3800, AUSTRALIA

[5]Monash Centre for Synchrotron Science, Monash University, VIC 3800, AUSTRALIA

[6]SPring-8/JASRI, Sayo, Hyogo 679-5198, JAPAN

ABSTRACT

Lungs have been imaged with high contrast at high spatial and temporal resolution using synchrotron phase contrast x-ray imaging. These images are analysed using techniques derived from the discipline of particle image velocimetry. This analysis yields 2D and 3D spatially resolved motion information of airway motion. It is likely that this information will result in the detection of airway damage and disease.

1. BACKGROUND

Many vital processes in the human body are mechanically dynamic; that is, they involve motion. It follows directly from the critical importance of these dynamic systems that scientists and clinicians have a keen interest in studying not just the anatomy of physiological systems, but also their function. In the history of the development of medical imaging systems, there is a consistent trend of adapting modalities originally designed to measure anatomical structure to systems capable of performing physiologically functional capabilities (Fouras *et al*. 2009)

Most evident amongst the dynamic physiological processes is the motion of the diaphragm and lungs and the resultant flow of air. Additionally, diseases and dysfunction of this process result in one of the most significant medical problems of our time. Pulmonary disease, leading to respiratory failure, is one of the greatest causes of morbidity and mortality in humans. Chronic obstructive pulmonary disease is the 5th leading cause of death in humans, is currently present in 10% of the population, and its incidence is increasing at a much greater rate than the other leading causes of death (Pauwels *et al*. 2004). Similarly, respiratory failure is the greatest cause of morbidity and mortality in newborn infants, particularly those born very preterm, with many of the survivors (30%) developing complications that have significant implications for the respiratory health of the individual throughout the remainder of their life.

It is currently not possible to detect most forms of lung disease before it is clinically evident, making many of these diseases untreatable. However, a relatively common feature of many lung diseases, such as emphysema and pulmonary fibrosis, is a regional alteration to the distal airway structure leading to marked regional changes in lung tissue compliance. Thus, imaging techniques that are capable of detecting regional differences in tissue velocities across the lung during the respiratory cycle are likely to detect the early stages of lung disease.

2. INTRODUCTION

X-ray imaging is by far the most commonly used biomedical imaging modality. It is simple to use, has good spatial resolution (typically of the order of microns), and the resulting images are relatively easy to interpret. Unfortunately, conventional absorption X-ray images display poor contrast for soft tissues such as the lungs.

Amongst organs of the body, the lung is unique as the volume of the air-filled lung predominantly comprises air: approximately 80% at the end of expiration. As a result, there is marked phase contrast between the air-filled airways and the surrounding tissue structures, which predominantly comprise water. This feature, which makes the lung so difficult to image by other imaging modalities (i.e., MRI and ultrasound), makes the lung ideally suited for phase contrast imaging.

We gain additional image contrast by exploiting the coherence of synchrotron X-radiation. Light is refracted by the phase gradients that occur at the boundaries between objects, which interferes with non-refracted light, to produce a kind of in-line holographic image. This produces a characteristic edge enhancing effect with up to 100 more contrast than that of absorption contrast and spatial resolution of the order of 10 microns. Figure 1 shows two X-radiographs of the lower left segment of a rabbit lung. Figure 1 (a) is a standard X-radiograph (using absorption contrast) where the lung tissue is only just visible as a cloudy, bright region in the top and left of the image, created by the reduced absorption of the air in the lung relative to the surrounding tissue. A dramatic difference can be seen in Figure 1 (b) where fine details of the precise nature and position of the lung are clearly seen.

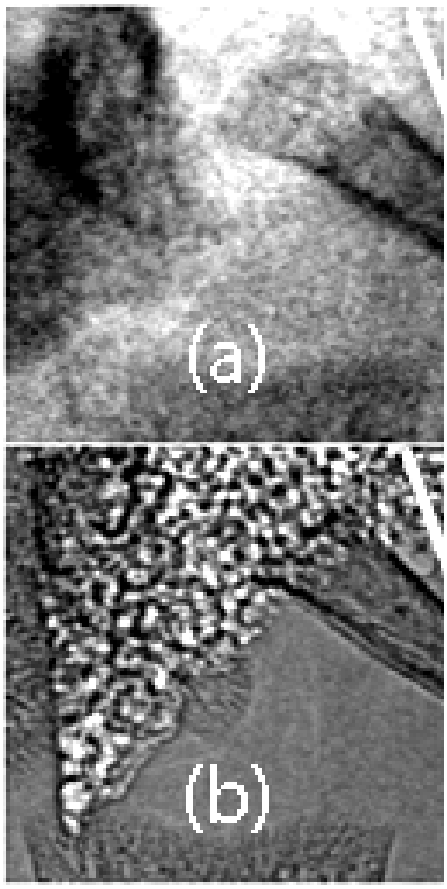

Figure 1. (a) Traditional (absorption contrast) X-ray image of the lower left portion of a rabbit lung. (b) Phase contrast image of the same lung acquired at the SPring-8 synchrotron. The images clearly show the increased contrast and the high resolution – with details at the scale of individual alveoli visible in figure (b).

With phase contrast, the aerated lungs usually appear as a speckled pattern comprising bright and dark dots (Figure 1b) (Kitchen *et al.* 2004). Initially these dots, or speckles, were thought to be individual alveoli as they exhibited similar dimensions to alveolar structures (Yagi *et al.* 1999). It was later realised that they could not be alveoli since tens to hundreds of them overlap within the lung (Lewis *et al.* 2003). In fact, it was demonstrated that lung speckle patterns arise from focusing effects, where overlapping airways act as aberrated compound refractive lenses (Kitchen *et al.* 2004). More recently, it has been demonstrated that the speckles created by these focussing effects faithfully follow the motion of the underlying structure that creates the speckle (Fouras *et al.* 2007, Irvine *et al.* 2008).

4. X-ray velocimetry

4.1 X-ray particle tracking

Recent publications have introduced X-ray particle tracking velocimetry (XPTV) (Seeger *et al.* 2001, Im *et al.* 2007). Seeger *et al.* (2001) measured particle displacements in bubble columns using particle tracking. A medical biplane X-ray source was used to image the particles from orthogonal perspectives allowing three components of velocity to be reconstructed. The measurements were severely limited in spatial and temporal resolution due to limitations in the imaging equipment and the low seeding density necessary to resolve individual particles. Im *et al.* (2007) used synchrotron X-ray imaging and particle tracking techniques to measure flow in a tube. This technique represents significant advances in both imaging and image processing over previous X-ray velocimetry methods. However, the velocity reconstruction method used is only applicable to axisymmetric flows in axisymmetric geometries. Furthermore, all particle tracking techniques are limited by the dual requirement that particles can be individually identified in not one, but at least two imaging frames. In X-ray illuminated flows, where the velocity may vary throughout regions of three-dimensional space that is mapped onto a single location in an image, this becomes a highly complex and severely restricting limitation.

4.2 X-ray particle image velocimetry (PIV)

PIV is a newer flow measurement technique than PTV, however, it is well established within the field of fluid mechanics (Adrian 1991, Adrian 2005). PIV has been shown to be capable of accurately measuring instantaneous velocity fields that have a high dynamic range. PIV differs from PTV mainly in that images are discretised and velocity measurements are performed statistically through the use of 2D cross-correlation functions. This significantly increases the robustness of the technique. There is no upper limit on tracers as there is no requirement to identify individual tracers in any sense and the addition of more tracers to images monotonically increases the signal to noise ratio. Furthermore, as a statistical measure, cross–correlation is robust and not sensitive to noisy data.

PIV has been combined with X-ray imaging by at least two groups in recent years (Lee & Kim 2003, Fouras *et al.* 2007). The penetrating ability of X-rays allows flow to be measured within opaque objects, with applications for non-invasive, high resolution blood flow field measurements. Figure 2 shows a schematic diagram of the imaging setup for x-ray PIV.

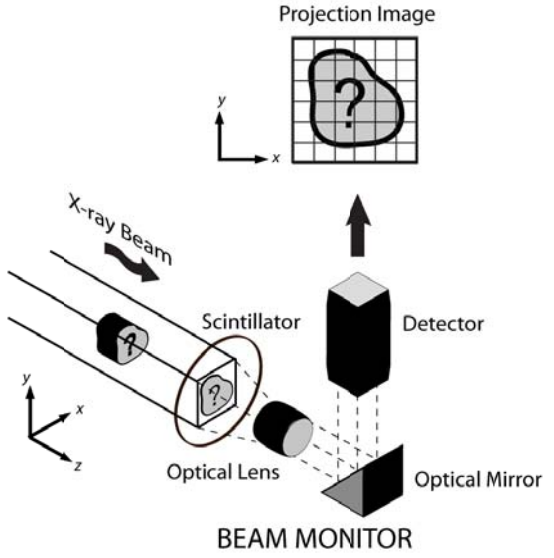

Figure 2. Schema of the configuration used to capture image data from the synchrotron experiments described in this paper. Note that X-rays are converted to visible light using a scintillator, which is in turn imaged by a visible light camera through a lens.

Lee & Kim (2003) measured flow in tubes with particles, and blood cells as tracer particles (Kim & Lee, 2006) using X-ray PIV. The methods described in these studies are limited to two components of the average velocity within the measurement volume. These authors use traditional PIV algorithm designed for optical/laser based velocimetry. These algorithms assume pulsed (instantaneous) illumination and zero out-of-plane flow gradients and therefore fail to take into account the three dimensional characteristics of X-ray imaging real flows. This results in a significant underestimation of flow velocity. Fouras *et al.* (2007) corrected this problem through the use of an algorithm that spans three frames rather than two and extrapolates the cross-correlation functions to the correct or ideal function. This results in a highly accurate high resolution measurement of velocity data.

5. METHODS

Experiments have been conducted measuring the patterns of motion of mechanically ventilated animal lungs. Two models have been used: newborn rabbit pups (both term and pre-term) as well as adult mice (without and without pulmonary fibrosis).

Animals were anaesthetised and ventilated, allowing complete control of airway pressures and inspiration and expiration periods. Animals were placed, head out, in a plethysmograph – a water bath, exploiting Archimede's Principle – to measure changes in lung volume simultaneously with X-ray imaging. Image acquisition was performed using a configuration similar to that described in Figure 2.

Data were acquired at the BL20B2 beamline at the SPring8 synchrotron (Japan), under time granted to the authors by the SPring-8 Program Review Committee (proposal nos. 2006B0002, 2007A0002). All images were acquired with a photon energy of 25keV. The camera system used was a Hamamatsu EMCCD, with a CCD array of 1280x1024 pixels, a maximum frame rate (at full resolution) of 30 frames per second and a bit depth of 12 bits per pixel. While more sophisticated 3D PIV results have been achieved, (using techniques described in Fouras *et al.* 2007, Irvine *et al.* 2008 and Dubsky *et al.* 2008), only the preliminary 2D results are shown here. These 2D results are derived using the PIV processing method described as the base technique in (Fouras *et al*. 2008)

In all cases, animals were treated ethically, with treatment protocols approved by ethics committees at both Monash University and the SPring8 synchrotron.

6. RESULTS

A considerable number of experiments have been conducted validating the PIV measurements. These validations have included adjustment of ventilator settings and comparison of 2D and 3D vector fields with those settings and volume measurements taken from plethysmograph measurements. In all cases the data have been shown to match ventilator settings to a high degree of sensitivity. Figure 3 shows typical PIV measurements of lung motion in a rabbit pup (29 days gestation), during inspiration (left) and expiration (right). The figure clearly shows considerable differences between the biomechanics of inspiration and expiration. This information is already proving useful in the design of ventilators for preterm children and their use in a clinical setting.

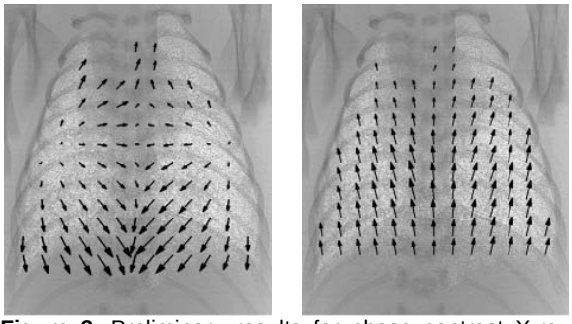

Figure 3. Preliminary results for phase contrast X-ray velocimetry data of the motion of a rabbit lung during: mid inspiration (left); and mid expiration (right); superimposed with images from which they were evaluated. Only ¼ of available motion vectors are shown to improve clarity of figure.

This system has also been used on adult mice to investigate the effects of pulmonary fibrosis on lung motion. Figure 4 shows preliminary 2D results for phase contrast X-ray velocimetry data of the motion of mouse lungs for a control mouse (top) and a mouse with pulmonary fibrosis (bottom). The first column of data represents 80ms after the start of inspiration, the middle column 120ms and the right column 320ms after inspiration.

While there are significant variations from any single animal to another, a clear difference in the vector patterns can be seen between the control mouse and the mouse with diagnosed pulmonary fibrosis. There is both an apparent phase lag between inspirations and a reduced magnitude of lung motion. Given that the fibrosis was not at all visible in the raw x-ray images, its detection via velocimetry is highly significant.

7. CONCLUSIONS

The authors have significantly adapted the use of medical x-ray images from purely anatomical imaging to a functional imaging modality. Lungs have been imaged with high contrast at high spatial and temporal resolution using synchrotron phase contrast x-ray imaging. These images are analysed using techniques derived from the discipline of particle image velocimetry. This analysis yields 2D and 3D spatially resolved motion information of airway motion. It is likely that this information will result in the detection of airway damage and disease.

Significant differences in the regional patterns of motion have been detected during the inspiration and expiration phases of the mechanical ventilation of term and preterm rabbit pups. Additionally, when measuring the patterns of motion in adult mouse lungs using PIV, significant differences are evident between control mice and those with pulmonary fibrosis.

ACKNOWLEDGMENTS

This research was supported by the Australian Research Council (Discovery Grant DP0877327) and the Australian National Health and Medical Research Council (Project Grant 491103). The authors also gratefully acknowledge the support provided by the SPring-8 synchrotron facility (Japan), which was granted by the SPring-8 Program Review Committee (proposal nos. 2006B0002, 2007A0002).

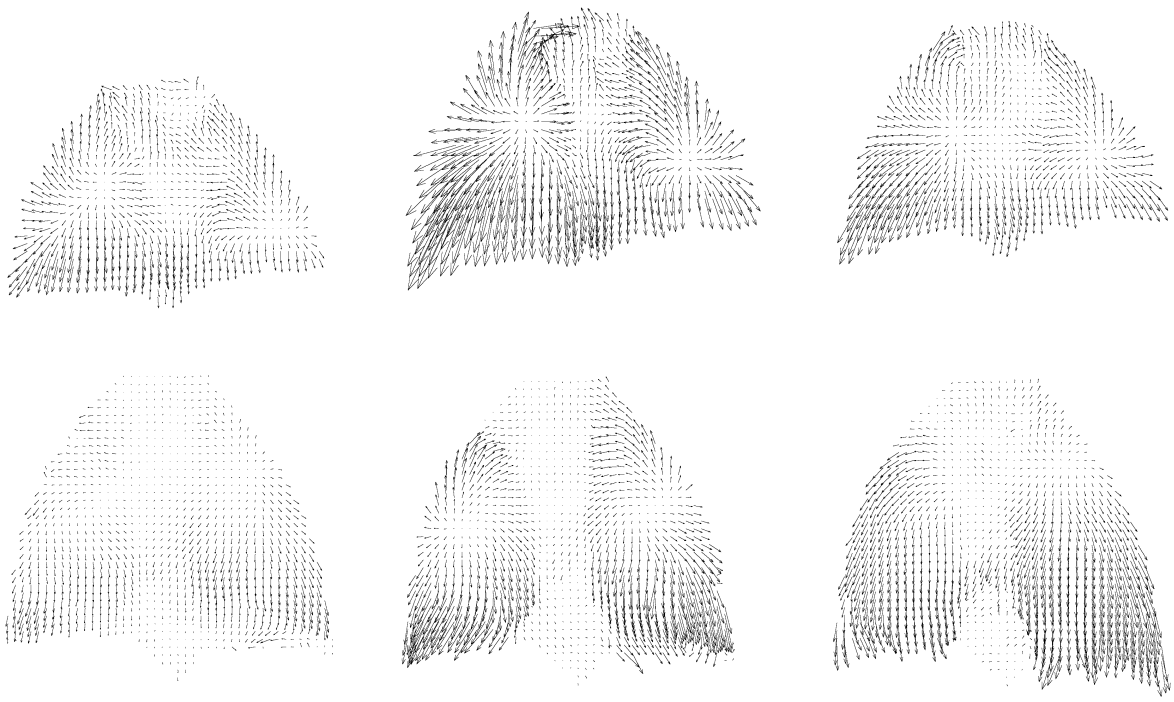

Figure 3. Preliminary results for phase contrast X-ray velocimetry data of the motion of mouse lungs for: (top) control mouse; (bottom) mouse with pulmonary fibrosis. Data are displayed in columns representing the same moment in the breathing cycle: (first col) 80ms; (mid col) 120ms and (right col) 320ms after start of inspiration.

REFERENCES

[1] Adrian R.J. (2005) Twenty years of particle image velocimetry. *Experiments in Fluids*, 39:159–169.

[2] Adrian R.J., (1991) Practical-imaging techniques for experimental fluid-mechanics. *Annual Review of Fluid Mechanics.* 23:261-304.

[3] Dubsky, S., Fouras, A., Irvine, S.C., Siu, K.K.W. & Hourigan, K., (2008) Three component, three-dimensional X-ray particle image velocimetry using multiple projections, 14th International Symposium on Applications of Laser Techniques to Fluid Mechanics, Lisbon, Portugal.

[4] Kitchen M.J., Paganin D., Lewis R.A., Yagi N., Uesugi K., and Mudie S.T. (2004) On the origin of speckle in X-ray phase contrast images of lung tissue. *Physics in Medicine & Biology*, 49(18): p. 4335-48.

[5] Fouras A., Dusting J., Lewis R. & Hourigan K., (2007) Three-dimensional synchrotron X-ray particle image velocimetry, Journal of Applied Physics, 102, 064916

[6] Fouras A., Lo Jacono D. & Hourigan K. (2008) Target-free stereo PIV: A novel technique with inherent error estimation and improved accuracy. *Experiments in Fluids*, 44(2), 317-329.

[7] Fouras A., Kitchen M.J., Dubsky S., Lewis R.A., Hooper S., and Hourigan K. (2009) The past, present and future of X-ray technology for *in vivo* imaging of function and form. *Journal of Applied Physics*, 105:102009.

[8] Im K.S., Fezzaa K., Wang Y.J., Lui X., and Lai MC. (2007), Particle tracking velocimetry using fast X-ray phase-contrast imaging. *Applied Physics Letters*, 90(9).

[9] Irvine S.C., Paganin D.M., Dubsky S., Lewis R.A. & Fouras A. (2008) Phase retrieval for improved 3-D velocimetric analysis of X-ray blood flow speckle patterns, *Applied Physics Letters*, 93(15), 153901.

[10] Kim G.B. and Lee S.J. (2007) X-ray PIV measurements of blood flows without tracer particles. *Experiments in Fluids*, 41:195–200.

[11] Lee S.J. and Kim G.B. (2003) X-ray particle image velocimetry for measuring quantitative flow information inside opaque objects. *Journal of Applied Physics*, 94:3620–3623.

[12] Lewis R.A., Hall C.J., Hufton A.P., Evans S., Menk R.H., Arfelli F., Rigon L., Tromba G., Dance D.R., Ellis I.O., Evans A., Jacobs E., Pinder S.E., Rogers K.D., (2003) X-ray refraction effects: application to the imaging of biological tissues *British Journal of Radiology*, 76: p. 301-8.

[13] Pauwels R.A., Rabe K.F., (2004) Burden and clinical features of chronic obstructive pulmonary disease (COPD). *LANCET* 364 (9434), 613-620.

[14] Seeger A., Affeld K., Goubergrits L., Kertzscher U., Wellnhofer E. (2001) X-ray based assessment of the three-dimensional velocity of the liquid phase in a bubble column. *Experiments in fluids* 31:193-201.

[15] Yagi, N., Y. Suzuki, K. Umetani, I., Kohmura, K. Yamasaki (1999) Refraction-enhanced x-ray imaging of mouse lung using synchrotron radiation source, *Medical. Physics*, 26(10): p. 2190-3.